A Novel Millimeter-Wave-Band Radio-Over-Fiber System With Dense Wavelength-Division Multiplexing Bus Architecture

Xiupu Zhang, *Member, IEEE*, Baozhu Liu, Jianping Yao, *Senior, IEEE*, Ke Wu, *Fellow, IEEE*, and Raman Kashyap

***Abstract*—In this paper, we propose a novel millimeter-wave-band radio-over-fiber (RoF) system with a dense wavelength-division multiplexing (DWDM) bus architecture. Two lasers with a small wavelength difference, phase locked and polarization aligned, are allocated at a central station (CS) for connecting the CS and each base station (BS), one laser for transmitting and the other for detection (the remote local oscillator). For the conceptual illustration, we consider a DWDM RoF system with a channel spacing of 12.5 GHz and RF of ~30-GHz millimeter-wave band. In the downlink system, a single-sideband (SSB) subcarrier is used with low RF imposed on an optical carrier at the CS, and an millimeter-wave-band RF signal is obtained at each BS using direct photodetection by the SSB subcarrier beat with the remote oscillator. In the uplink system, the received millimeter-wave-band RF signal at each BS is imposed on the two optical carriers simultaneously, one optical carrier with the closest SSB subcarrier is optically filtered out and fed into in the uplink transmission fiber without frequency interleaving; the electrical signal with a low IF can be photodetected directly at the CS. Such an RoF system has simple, cost-effective, and maintenance-reduced BSs, and is immune to laser phase noise in principle.**

***Index Terms*—Access networks, millimeter-wave communications, optical fiber communications, radio-over-fiber (RoF), subcarrier modulation, wavelength-division multiplexing.**

I. Introduction

In ORDER to provide broad-band service in local wireless access networks, exploring where the RF can be allocated with a large amount of bandwidth to implement broad-band services has been explored across the world [1]. Due to the limited availability of the RF bands, the fourth generation of wireless access systems would be moved to millimeter-wave band. However, cost-effective technology and systems have to be developed to deliver the millimeter-wave-band signals. The hybrid radio-over-fiber (RoF) system has been studied for many years as a promising technique for providing wireless broad-band service [2]–[24]. The advantage of the RoF system is that complicated signal processing can be localized at the central station (CS), rather than allocated to a number of remote base stations (BSs). Such a system can make the CS more complicated and allow the BSs to share resources with the CS, thereby simplifying the architecture and reducing the complexity of the BSs. The remote BSs with the small millimeter-wave-band coverage such as picocell will significantly result in an increase of the number of BSs, thus the implementation of the simple, compact, and maintenance-reduced BSs in terms of cost is required. Therefore, a number of RoF design techniques have been proposed and investigated to explore cost-effective RoF systems. For example, a technique for sharing a light source for both downlink and uplink systems was proposed, thereby requiring no lasers installed at BSs and, thus, the BSs are cost effective and maintenance reduced [2]–[4].

As RoF systems may be degraded by fiber chromatic dispersion, the single-sideband (SSB) subcarrier modulation technique was proposed and demonstrated as a solution to overcome this effect [5], [6]. In other words, either the lower sideband (LSB) or the upper sideband (USB) subcarrier is only used for transmission. Subcarrier modulation can be obtained by either direct or external modulation. However, for external modulation, an intensity modulator like a Mach–Zehnder modulator (MZM) or an electro-absorption modulator (EAM) is often used to generate SSB subcarriers to overcome the effect of frequency chirp and nonlinear response of lasers. Moreover, EAMs can be polarization insensitive, which makes the techniques of the sharing of light sources and/or remote local oscillators possible.

Due to the architectural characteristics of millimeter-wave-band RoF systems, a larger number of BSs are connected to a CS via fiber. Hence, the dense wavelength division multiplexing (DWDM) technique is a strong candidate to better support the connections between CSs and BSs with simply one wavelength for each BS. Thus, application of the DWDM in RoF systems has been extensively investigated [8]–[23]. However, when DWDM techniques are applied for RoF systems, some technical issues arise due to the use of subcarrier modulation in RoF systems. The millimeter-wave-band subcarriers are separated by tens of gigahertz from the optical carrier, which is usually beyond the DWDM channel spacing and, therefore, the bandwidth of DWDM multiplexers and demultiplexers. Therefore, conventional optical multiplexers and demultiplexers, which are commercially available and used for current DWDM transmission systems, may not be used directly for millimeter-wave-band RoF systems. One straightforward technique is to use a specially designed optical multiplexer or demultiplexer, which separately combines or extracts each optical carrier and its

Manuscript received April 1, 2005; revised September 21, 2005. This work was supported in part by the Canadian Institute for Photonics Innovations.

X. Zhang and B. Liu are with the Department of Electrical and Computer Engineering, Concordia University, Montréal, QC, Canada H3G 1M8 (e-mail:xzhang@ece.concordia.ca).

J. Yao is with the Microwave Photonics Research Laboratory, School of Information Technology and Engineering, University of Ottawa, Ottawa, ON, Canada K1N 6N5.

K. Wu and R. Kashyap are with the Poly-Grames Research Center, Départment de Génie Electrique, École Polytechnique de Montréal, Montréal, QC, Canada H3T 1J4.

Digital Object Identifier 10.1109/TMTT.2005.863045

millimeter-wave-band subcarriers [8]; thus, the current commercially available optical multiplexers/demultiplexers cannot be used, increasing the resulting cost. A second technique is to up-shift RFs at BSs for downlink systems, accomplished in the optical domain with a remote pilot tone [3], [9], [10], or in the electrical domain with electrical mixers and voltage-controlled oscillators combined with a remote pilot tone [11]. A third technique is called the frequency-interleaved DWDM [12], [13]; in order to demultiplex each optical carrier together with its subcarriers at CSs, the dual-mode light is used at the CSs for each optical channel to beat with the desired subcarriers for generating IF signals with an optical coherent heterodyne detection. This technique is possible to be used for uplink systems, but is not a good one for downlink systems, as the complexity of BSs is increased, conflicting with the objective of the simple and maintenance-reduced BSs. In addition, the two wavelength interval of the dual-mode local-oscillator source has to be tuned accurately to ensure it beats with the desired optical carrier and corresponding subcarrier with polarization control. A fourth technique is to use photonic frequency down-conversion [14] for uplink systems in which the optical carrier and its subcarriers are divided into two parts by carrier-suppressed modulation with an MZM at CSs to down-shift optical carriers before optical demultiplexing; however, this technique is also applicable only for uplink systems besides the complicated frequency down-conversion.

In this paper, we propose a novel RoF system for the DWDM bus architecture. With this architecture, millimeter-wave-band RF signals (15–60 GHz) can be directly generated optically in downlink systems at BSs, and IF signals (2–10 GHz) can be directly obtained optically in uplink systems at CSs. The BSs is shown to be very simple and maintenance significantly reduced because the electrical system at each BS consists of only power supply, electrical amplifiers, and electrical filters. In uplink systems, a millimeter-wave-band signal is imposed directly onto two optical carriers simultaneously at each BS, and one along with one subcarrier, which is ∼2–10 GHz away from that optical carrier are filtered out optically; they are fed into the uplink transmission fiber without frequency interleaving. The conventional optical demultiplexer directly filters out each optical carrier with its subcarrier for each channel; thus, a low IF signal is obtained at the CS by direct photodetection. The existing DWDM multiplexers and demultiplexers can be still utilized for both downlink and uplink systems, as the optical carriers and their subcarriers are not frequency interleaved.

We will illustrate this RoF system for a DWDM bus architecture with a channel spacing of 12.5- and ∼30-GHz band RF signals. The basic idea of our proposed RoF system is based on the principle that the optical carrier, which was used for carrying a subcarrier in transmission, is replaced by the other optical carrier, which is also located at the CSs acting for a remote local-oscillator laser. In other words, for each RoF system, two optical carriers are used, one for transmitting and the other for detection. This technique can be easily migrated to DWDM with a channel spacing of 25 GHz and each optical carrier having multiple subcarriers, as well as other millimeter-wave RF bands. For the conceptual proof of principle, an RoF system with one CS and one BS is verified by simulation on an OptSim platform, and each optical carrier conveys one differential phase-shift keying (DPSK) subcarrier signal at 155.52 Mb/s over 25 km of a single-mode fiber (SMF) for both downlink and uplink systems.

II. Proposed System for Bus Architecture

We assume that an RoF system with the bus architecture consists of two fiber links: one for the downlink and the other for the uplink. A key to DWDM access networks is to use wavelengths for the connections between a CS and BSs, and the CS and each BS is connected using one wavelength channel.

In the downlink system, as shown in Fig. 1, there are a total of n optical channels or carriers, i.e., $C_1, C_2, C_3, \ldots, C_n$ or, in terms of wavelengths, $\lambda_1, \lambda_2, \lambda_3, \ldots, \lambda_n$. In this illustration, we only consider each optical carrier transporting one subcarrier, located at the LSB of the optical carrier. The LSB subcarrier can be obtained by using an EAM driven by an RF signal with a low RF RF'_{d1}, as shown in Fig. 1. For example, consider $\mathrm{RF}'_{d1} = 4$ GHz, thus the total occupied bandwidth including the optical carrier and subcarrier is ∼4 GHz for each channel, far below the channel spacing of 12.5 GHz. Therefore, conventional optical multiplexers can be used for this downlink system. There is the other set of optical carriers, i.e., $C'_1, C'_2, C'_3, \ldots, C'_n$ or, in terms of wavelengths, $\lambda'_1, \lambda'_2, \lambda'_3, \ldots, \lambda'_n$, which are continuous wave (CW) and 25 GHz shorter in wavelength (or higher in frequency); these are optically multiplexed and coupled together with the first set of optical channels, as shown in Fig. 1. Suppose that the optical carriers λ_1 and λ'_1, λ_2, and λ'_2, and so on are phase locked, respectively; and the two optical carriers (i.e., λ_1 and λ'_1, λ_2, and λ'_2, and so on) have the same polarization states, respectively, until they are combined together. Fig. 2 shows the optical spectrum after the optical combiner (i.e., at the position A_2 in Fig. 1). All optical carriers and subcarriers transmit over the downlink fiber with a length X_i, where i denotes the number of BSs, $i = 1, 2, 3, \ldots$, and first arrive at BS 1 after transmission over a fiber length X_1; a fraction of optical power using a power splitter is directed to BS 1. In order to generate the ∼30-GHz RF signal, optical filter 1 is used to extract the optical carrier C'_1 and the subcarrier L_1, resulting in the optical spectrum shown in Fig. 2 (within dashed lines). Accordingly, all other BSs have the similar configuration as BS 1. The bandwidth of optical filter 1 is not so crucial, as the crosstalk is easily removed by electrical filtering and optical filtering is mainly used to limit optical saturation of photodiodes. Another optical filter (i.e., optical filter 2) is utilized to extract the optical carriers C_1 and C'_1 used for the uplink system. As shown in Fig. 2, 3-dB degradation of optical modulation depth (the power ratio of the optical carrier and its subcarrier in this paper) may be induced if a 3-dB coupler (i.e., coupler 1 in Fig. 1) is used to combine the two sets of the optical carriers, depending on the polarization of the two overlapped optical carriers. For example, consider the overlapped optical carriers C_1 and C'_3: no modulation depth degradation occurs if their polarization states are orthogonal.

Suppose that the optical components at BSs do not induce any polarization walkoff between both optical carriers C_1 and C'_1, C_2, and C'_2, and so on. The current, resulting from beat between the optical carrier C'_1 and the LSB subcarrier L_1, is given by [3]

$$i_{c1',L1}(t, X_1) \propto a_{c1'} \cdot a_{L1} \exp\left\{j\psi_{c1',L1}(t, X_1)\right\}. \qquad \text{(1a)}$$

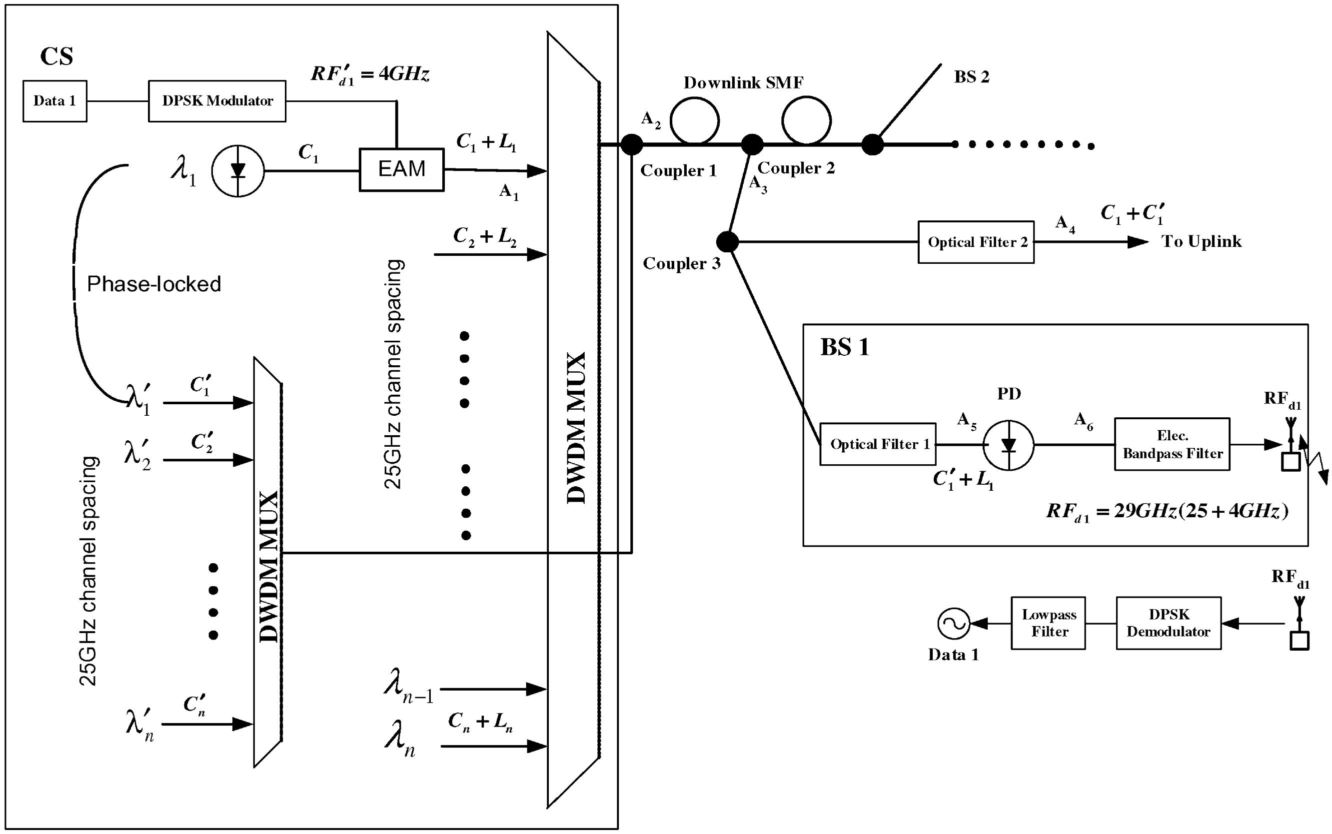

Fig. 1. Schematic illustration of the proposed RoF downlink system with the DWDM bus architecture. Photodiode: PD.

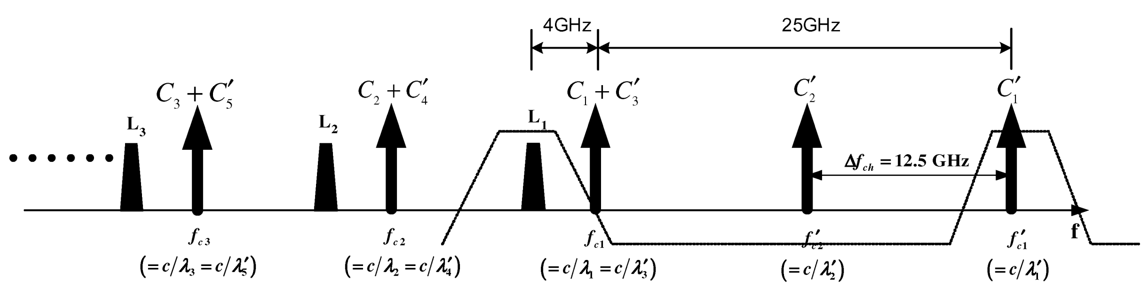

Fig. 2. Optical spectrum at the optical combiner 1 output (i.e., at the position A_2 in Fig. 1). The dashed line indicates optical filter 1 in Fig. 1.

In (1a), $a_{c1'}$ and a_{L1} represent the relative amplitudes of the optical carrier C'_1 and LSB subcarrier L_1. The propagation constant $\beta^{d,n}(f)$ for the nth downlink optical carrier is expressed by the Taylor series $\beta^{d,n}(f) \approx \beta_0^{d,n} + \beta_1^{d,n} \cdot 2\pi(f - f_{cn}) + (1/2)\beta_2^{d,n} \cdot \{2\pi(f - f_{cn})\}^2$, $\beta_1^{d,n}$, and $\beta_2^{d,n}$ are related to the group delay time, and group velocity dispersion (GVD), respectively, of the downlink fiber. The quantity $\psi_{c1',L1}(t, X_1)$ is given by

$$\begin{aligned}
&\psi_{c1',L1}(t, X_1) \\
&= 2\pi(f_{c1'} - f_{c1} + f_{L1})\left(t - \beta_1^{d,1'}X_1\right) \\
&\quad + \phi_{c1'}(t - \beta_1^{d,1'}X_1) - \phi_{c1}\left(t - \beta_1^{d,1}X_1\right) \\
&\quad + \theta_{L1}\left(t - \beta_1^{d,1}X_1\right) \\
&\quad + \frac{1}{2}\beta_2^{d,1} \cdot (2\pi f_{L1})^2 X_1 + \left[\beta_1^{d,1'} 2\pi(f_{c1'} - f_{c1}) \cdot X_1\right]
\end{aligned} \tag{1b}$$

where f_{cn} and $\phi_{cn}(t)$ are the optical carrier frequency and phase noise of the optical carriers $C'_1(n = 1')$ and $C_1(n = 1)$, and $f_{L1}(\theta_{L1}(t))$ is the RF (modulated signal phase) for the subcarrier L_1. For the channel spacing of 12.5 GHz, the frequency difference $f_{c1'} - f_{c1}$ is 25 GHz. If the subcarrier RF around $\sim$4 GHz is used, the beat frequency between the optical carrier C'_1 and the LSB subcarrier L_1 is $\sim$29 GHz. Thus, the $\sim$4-GHz subcarrier at the CS is up-shifted to the $\sim$29-GHz RF signal at the BSs. Compared to the conventional coherent heterodyne detection, the optical carrier C'_1 acts as the local oscillator for the subcarrier L_1. The $\sim$29-GHz RF signal is finally launched into air by an antenna after electrical filtering. If the payload contains a DPSK signal, the user simply decodes the DPSK signal by an electrical DPSK demodulator and a low-pass filter. Since the SSB technique is used, the fiber GVD does not introduce any distortion, as shown in (1b). Moreover, note that the terms $\phi_{c1'}(t - \beta_1^{d,1'}X_1) - \phi_{c1}(t - \beta_1^{d,1}X_1)$ in (1b), which is the laser

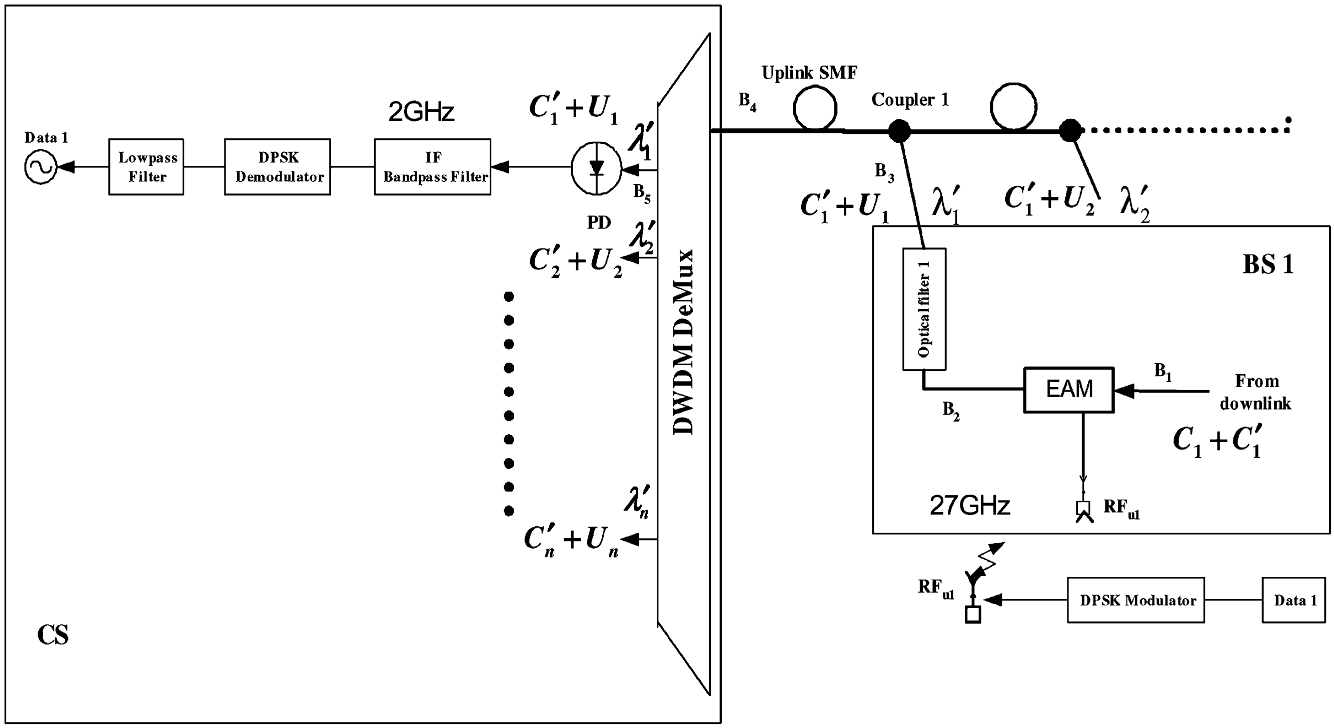

Fig. 3. Schematic illustration of the proposed RoF uplink system with a DWDM bus architecture.

phase noise from the optical carriers C_1' and C_1, can be cancelled because the two lasers are phase locked. Therefore, the downlink system can be immune to laser phase noise.

A small RF adjustment around $\sim$30 GHz at the BSs can be easily obtained by a small shift of the subcarrier RF at the CS. For a large RF change, the optical filter 1 at BSs and/or the other set of optical carriers (i.e., $\lambda_1', \lambda_2', \lambda_3', \ldots, \lambda_n'$) at the CS must be changed. As shown in Fig. 2, if optical filter 1 extracts the optical carrier C_2' and L_1, an RF around $\sim$15 GHz can be obtained. Similarly, an RF around $\sim$60 GHz can also be obtained by shifting λ_1' further shorter. An optical carrier with multiple subcarriers and a channel spacing of 25 GHz, as shown in [11], can be also applied to our proposed RoF system. Furthermore, in our proposed optical demultiplexing technique, shown in Fig. 2, the optical modulation depth can be easily improved by reducing the optical carrier's power by increasing insertion loss of optical filter 1 at the optical carrier, thus the performance of the downlink systems can be improved [24].

The proposed uplink RoF system is illustrated in Fig. 3. To simplify BSs and reduce maintenance of the BSs, the remote oscillator source technique is used as in [2]–[4]. For example, the optical carriers with the optical wavelengths λ_1 and λ_1' are used for both downlink and uplink systems for the connection between the CS and BS 1. The $\sim$27-GHz RF signal, which is received from an antenna, is imposed onto the two optical carriers C_1 and C_1' simultaneously by using a polarization-insensitive EAM, as shown in Fig. 3, at BS 1. Thus, each of the optical carriers C_1 and C_1' has two subcarriers; and an optical filter (i.e., optical filter 1 in Fig. 3) simply filters out the optical carrier C_1' and subcarrier U_1, which is a subcarrier of the optical carrier C_1; therefore, the optical carrier C_1' becomes the new optical carrier for the subcarrier U_1. The optical carrier C_1' and subcarrier U_1 are then coupled into the uplink transmission fiber. Optical filtering also reduces nonadjacent channel crosstalk. Since the frequency difference between the optical carrier C_1' and subcarrier U_1 is $\sim$2 GHz, the conventional DWDM demultiplexer can then be directly applied to extract each optical carrier together with its subcarrier. Moreover, frequency interleaving is not used and, thus, optical signal to noise ratio (OSNR) penalty and modulation depth degradation due to the frequency interleaving are not introduced. The optical spectrum at the input of the DWDM demultiplexer is shown in Fig. 4. Alternatively, optical filter 1 can extract the optical carrier C_1 and subcarrier U_1'; thus, the optical carrier C_1 is still used for the uplink transmission, not just for the downlink. We consider the optical carrier C_1' and subcarriers U_1 as an example. The signal current after photodetection can be expressed by

$$i_{c1',U1}(t, 2X_1) \propto b_{c1'} b_{U1} \exp\left[j\psi_{c1',U1}(t, 2X_1)\right] \tag{2a}$$

where $\psi_{c1',U1}(t, 2X_1)$ is given by

$$\begin{aligned}
&\psi_{c1',U1}(t, 2X_1)\\
&\quad\approx 2\pi(f_{c1'} - f_{c1} - f_{U1})\Big(t - 2\beta_1^{d,1} X_1\Big)\\
&\qquad + \phi_{c1'}\left(t - 2\beta_1^{d,1} X_1\right) - \phi_{c1}\left(t - 2\beta_1^{d,1} X_1\right)\\
&\qquad + \theta_{U1}\left(t - \beta_1^{d,1} X_1\right)\\
&\qquad + \frac{1}{2}\beta_2^{d,1} \cdot \{2\pi(f_{U1})\}^2 \cdot X_1 + \beta_1^{d,1} 2\pi f_{U1} \cdot X_1\\
&\qquad + 2\beta_1^{d,1} \cdot 2\pi(f_{c1'} - f_{c1}) \cdot X_1
\end{aligned} \tag{2b}$$

where the Taylor' series coefficients of the uplink propagation constant at the optical carrier C_1' were assumed to be the same

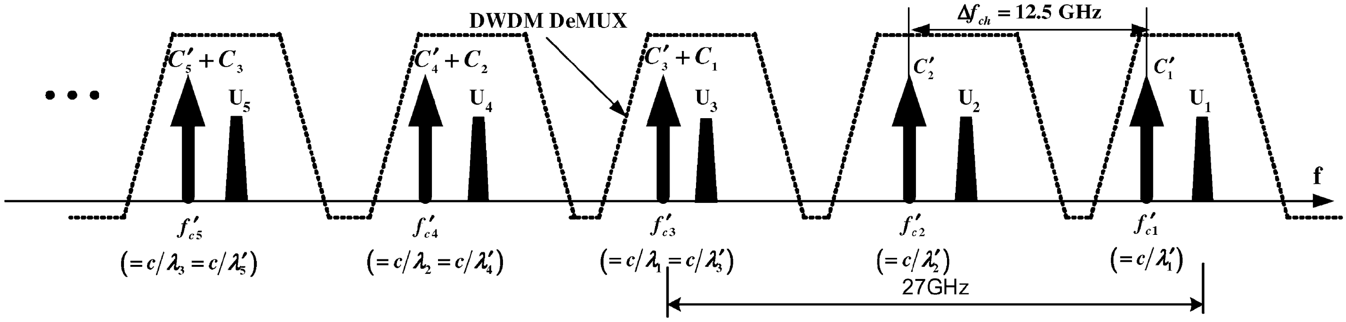

Fig. 4. Optical spectrum of the uplink system at the input of the DWDM demultiplexer (i.e., at the position B_4 in Fig. 3). The dashed line indicates DWDM demux in Fig. 3.

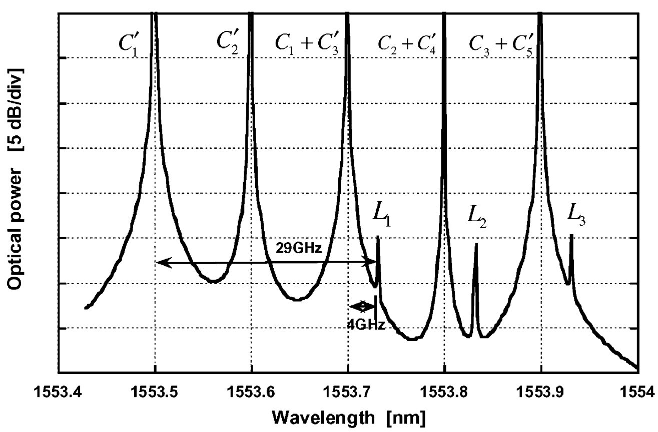

Fig. 5. Optical spectrum at the DWDM multiplexer output (at the position A_2 of Fig. 1).

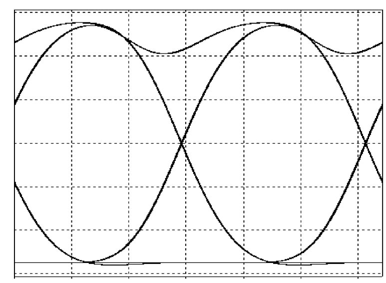

Fig. 6. Eye diagram for recovered 155.52-Mb/s signal from the LSB subcarrier L_1.

as those for the optical carrier C_1. In (2a), $b_{c1'}$ and b_{U1} represent the relative amplitudes of the optical carrier C'_1 and USB subcarrier U_1. In (2b), $f_{U1}(\theta_{U1}(t))$ is the RF (modulated signal phase) of the USB subcarrier U_1 related to the optical carrier C'_1. After IF electrical bandpass filtering, the IF signal is sent to the DPSK demodulators to recover the users' data. Note that the laser phase-noise terms $\phi_{c1'}(t - 2\beta_1^{d,1}X_1) - \phi_{c1}(t - 2\beta_1^{d,1}X_1)$ can be cancelled because the two lasers are phase locked. Hence, the uplink system can also be immune to laser phase noise.

III. Verification by Simulation

The downlink system configuration is almost the same as in Fig. 1, with one CS and one BS. Five optical carriers with DWDM channel spacing of 12.5 GHz and wavelengths of $\lambda'_1 = 1553.5$ nm, $\lambda'_2 = 1553.6$ nm, $\lambda_1 = 1553.7$ nm, $\lambda_2 = 1553.8$ nm, and $\lambda_3 = 1553.9$ nm are used in our simulation. The optical transmitter at the CS for the optical carriers C_1, C_2, and C_3 consists of a CW laser source, and an EAM driven by one DPSK modulated signal at 155.52 Mb/s with an RF carrier of 4 GHz. To obtain an optical LSB subcarrier, an optical notch filter is used after the EAM to remove the USB subcarrier. A DWDM multiplexer combines all the optical carriers and their subcarriers together, resulting in an optical spectrum shown in Fig. 5, and further sent to BS 1 via a 25-km downlink SMF link. A 3-dB optical coupler is used to drop a fraction of optical power to BS 1, then 90% of which is reserved for the uplink system and 10% of which is passed to the downlink photodetection. At BS 1, the three adjacent optical carriers C'_1, C'_2, and $C_1 + C'_3$ and one subcarrier L_1 are extracted by an optical filter with a center wavelength of 1553.79 nm and a bandwidth of $\sim$30 GHz; the undesired optical carriers are removed by an optical notch filter. After photodetection, the beat by the optical carrier C'_1 (1553.5 nm) with the LSB subcarrier L_1 (1553.74 nm) generates an RF current at $\sim$29 GHz. The user receives the recovered data after DPSK demodulation. The eye diagram for the recovered data is shown in Fig. 6. It is seen that interference occurs at bit "1." This may be because optical carriers C'_2 and $C_1 + C'_3$ are not completely suppressed by optical filter 1 in Fig. 2, thus, interference due to beats between the residual optical carrier C'_2 or $C_1 + C'_3$ and the subcarrier L_1 is introduced.

In the uplink RoF system, BS 1, as shown in Fig. 3, is considered without local oscillator lasers. An optical filter at BS 1 is used to obtain the optical carriers at the wavelengths of $\lambda'_1 = 1553.5$ and $\lambda_1 = 1553.7$ nm from the downlink system, which are injected into an EAM. The RF signal received at a RF of 27 GHz at BS 1 directly drives the EAM; thus, each optical carrier has two subcarriers, as shown in Fig. 7.

An optical filter (i.e., optical filter 1) is used to filter out the optical carrier C'_1 and subcarrier U_1, as shown in Fig. 7; they are hand fed into the uplink transmission fiber. Since the optical carrier C'_1 has a frequency separation of $\sim$2 GHz from the USB subcarrier U_1, a conventional DWDM demultiplexer with a channel spacing of 12.5 GHz can directly extract each optical carrier and its subcarrier for all channels. By photodetection, a current with IF at $\sim$2 GHz is obtained. The current is sent to an electrical Butterworth filter with a central frequency of $\sim$2 GHz, resulting in an eye diagram shown in Fig. 8, and is finally decoded by an asynchronous DPSK demodulator. It is seen that in-

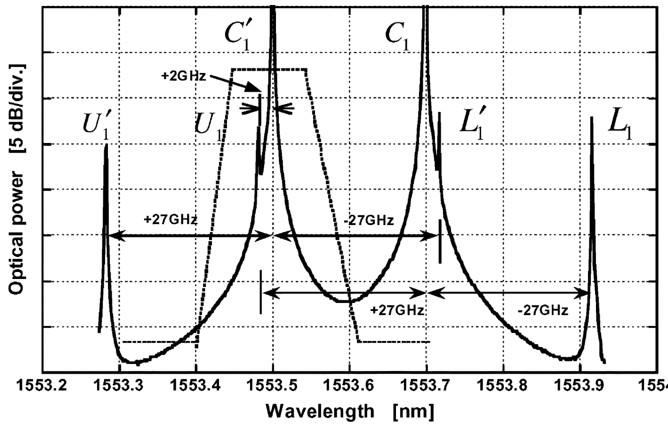

Fig. 7. Optical spectrum at the EAM output at BS 1. The dashed lines indicate optical filter 1 in Fig. 3.

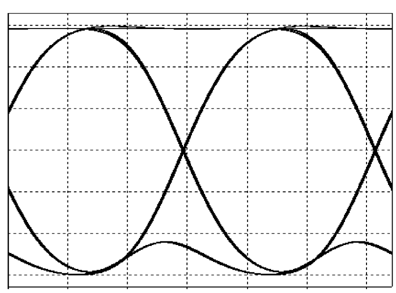

Fig. 8. Eye diagram for recovered 155.52-Mb/s signal from the USB subcarrier U_1.

terference occurs at bit "0." This is because the residual optical carrier C_1 beats with the subcarrier U_1, resulting in interference.

In both down- and up-links, we have used a small modulation index to avoid harmonic distortion due to nonlinear EAM modulation characteristics. The other system parameters used in the simulation are summarized in Table I.

TABLE I
SYSTEM PARAMETERS USED IN THE SIMULATION

items	downlink	uplink
DPSK data	155.52Mb/s at 2^{23}-1	
EAM mod. voltage	Bias: -3.5V, V_{pp}: 1 V	V_{pp}: 2 V
Modulation index 1)	28 dB	22 dB
RF or IF at CS	4 GHz	2 GHz
DWDM Mux 2)	12GHz, 35dB	-
DWDM Demux 2)	-	12GHz, 35dB
Channel spacing	12.5GHz	
Fiber loss	0.21 dB/km	
Fiber dispersion	16 ps/(nm-km)	
Fiber length	25 km	
Optical filter 1 2)	A bandpass filter (33GHz, 35dB) & a notch filter (25GHz, 35dB)	A bandpass filter (10GHz, 35dB)
Optical filter 2 2)	Two bandpass filters (4GHz, 35dB)	
Elec. Bandpass filter	5th Butterworth (0.6GHz)	
Elec. lowpass filter	5th Bessel (0.1GHz)	
Photodiodes	ideal	
RF at BS	29 GHz	27 GHz
Optical coupler 1	50/50%	10/90%
Optical coupler 2	90/10%	-
Optical coupler 3	90/10%	-

1). Modulation index is defined the ratio of optical carrier to its subcarrier.
2). They are 3-dB bandwidth in GHz and non-adjacent crosstalk in dB. All insertion loss of optical components is ignored.

IV. DISCUSSION

Polarization alignment between the optical carriers C_1' and C_1, C_2', and C_2, and so on before launching into the downlink transmission fiber is required for our proposed RoF system. The optical transmission path of optical carriers such as C_1' and C_1 with its subcarriers, launched with the same polarization states at the CS, is the same after optical combiner 1 in Fig. 1; and the polarization misalignment or walkoff of the optical carriers C_1 and C_1', as well as the subcarriers with a small frequency difference is possibly induced by transmission fiber and inline optical components. Due to polarization-mode dispersion, the differential group delay (DGD) between the optical carriers C_1' and C_1, as well as L_1 or U_1 will introduce fading in the beat signal. If the frequency between the optical carrier and its subcarrier is $\Delta\omega$, and the DGD of the fiber link is $\Delta\tau$, then the angle of separation of polarization states of these two frequency components on the Poincare sphere is $\Delta\alpha = \Delta\tau\Delta\omega$. The received subcarrier signal is $I(t) = A(t)\cos[\Delta\omega(t + \Delta\tau/2)] \cdot \cos(\Delta\tau\Delta\omega/2)$, where $A(t)$ is the signal carried by the subcarrier [25]. The factor of $\cos(\Delta\tau\Delta\omega/2)$ introduces fading due to the polarization walkoff. If we consider a frequency separation of 60 GHz and $\mathrm{DGD} = 1$ ps/km, the polarization walkoff is approximately 1.5° for 25-km fiber and 3° for 50-km fiber. Therefore, polarization walkoff in the transmission fiber hardly induces fading in our proposed RoF system. The other possibility for inducing polarization walkoff between the two optical carriers or the optical carrier and its subcarrier separated by, say, $\sim$60 GHz may be due to inline optical components such as optical filters at BSs. In [8], each optical carrier and its 60-GHz subcarrier are separately filtered out and then recombined optically; the detected signal does not show polarization misalignment or walkoff induced by the inline optical components. Moreover, in our proposed system, the optical carriers such as C_1 and C_1' pass the same inline optical components and, therefore, have the same polarization evolution. As shown in [11], an optical carrier and its subcarrier at a frequency of $\sim$23 GHz away from the optical carrier are optically extracted by two cascading fiber Bragg grating filters and a circulator, which has the same process as optical filters 1 and 2 in Figs. 1 and 3. It was shown that inline optical components do not introduce polarization walkoff between the optical carrier and its subcarrier. Therefore, the polarization walkoff of optical carriers C_n and $C_n' (i = 1, 2, 3, \ldots)$, as well as their subcarriers could be negligibly small in our proposed RoF system.

Since the two lasers for the optical carriers C_1 and C_1', C_2, and C_2', C_3, and C_3', and so on are phase locked, the beat between the optical carrier and their subcarrier, such as C_1'

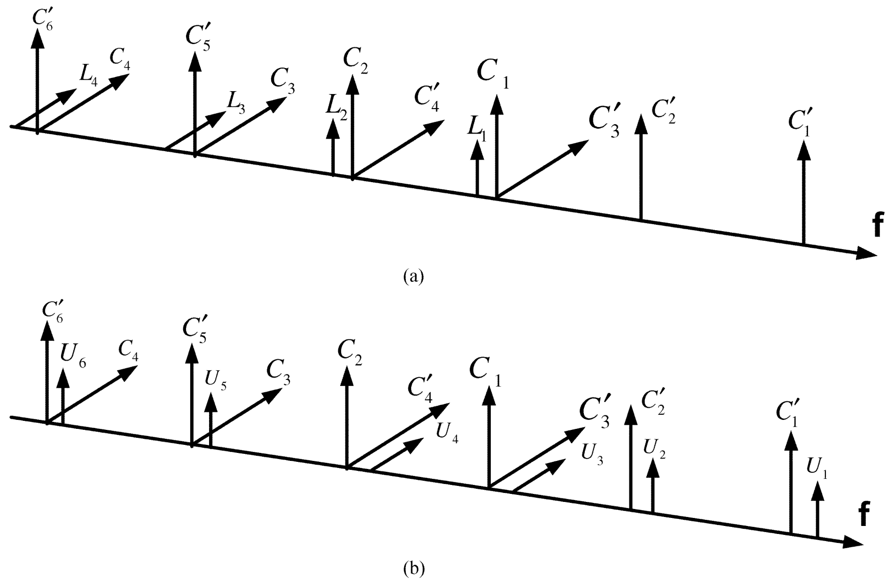

Fig. 9. Possible polarization orientation arrangement of two sets of optical carriers for: (a) the downlink and (b) the corresponding uplink.

with L_1, C'_2 and L_2, C'_3, and L_3, and so on for the downlink, or C'_1 with U_1, C'_2 with U_2, C'_3 with U_3, and so on for the uplink will cancel the impact of laser phase noise. However, starting from the wavelength of the optical carrier C_1, there is an overlapping optical carrier for each channel, as shown in Fig. 2. For example, the optical carrier C'_3 is overlapped with the optical carrier C_1; thus, the laser phase noise may degrade system performance because the optical carrier C_1 may beat with the subcarrier L_3 and the laser phase noise of the optical carriers C_1 and C'_3 cannot be cancelled in the downlink. In the uplink, as shown in Fig. 4, the optical carrier C'_3 is overlapped with the optical carrier C_1; the beat by the optical carrier C_1 with the subcarrier U_3 may occur so the laser phase noise of optical carriers C_1 and C'_3 cannot be cancelled and, thus, may degrade the uplink system as well.

Consequently, the overlapping optical carriers may introduce the degradation of optical modulation depth and laser phase-noise impact. One simple solution is to use the two sets of wavelengths with a nonoverlapping frequency offset. For example, for a channel spacing of 25 GHz, the two sets of the wavelengths have a 12.5-GHz offset and optically interleaved together instead of an optical combiner, such as λ_1 and λ'_3 having a difference of 12.5 GHz; but the spectral efficiency is degraded. A second solution is to use alternative polarization setting. For example, optical carriers C_1 and C'_3, C_2, and C'_4, and so on are orthogonal in polarization. Fig. 9 show a possible arrangement of optical carriers with an alternative polarization orientation for the downlink and uplink systems. With this arrangement, the proposed RoF system is immune to laser phase noise and has no optical modulation depth penalty because the optical carriers C_1 and C'_3, C_2, and C'_4, and so on are orthogonal in polarization.

Nevertheless, if the optical carriers C_1 and C'_3, C_2, and C'_4, and so on are overlapped in wavelength and not be orthogonal in polarization, then 3-dB degradation of OSNR and optical modulation depth may be introduced, but will not become a critical limit on the RoF systems. Moreover, the beat by the optical carrier C_1 with the subcarrier L_3 in the down-link or optical carrier C_1 and the subcarrier U_3 in the up-link only introduces one portion of the detected signal, which is deteriorated by laser phase noise, and the other portion is not impacted; therefore, laser phase noise may not be a limiting factor in our proposed RoF system either.

Conventionally phase locking of two lasers is complicated, particularly for lasers with wide linewidths. However, it was found recently that optical supercontinuum (SC) sources can be used for RoF systems and, more importantly, all SC modes are highly phase locked to one another [26]. Thus, if polarization-maintaining fiber is used for SC sources, all SC modes will have the same polarization orientation besides being phase locked. As shown in Fig. 9, two polarization maintaining SC sources can fulfill our proposed RoF systems for all channels. Another easy technique is to use a dual-mode laser for each channel, one for transmitting and the other for the remote oscillator. The dual modes are phase locked and polarization aligned [12].

Interference noise may be introduced in our proposed system. In both downlink and uplink, optical filter 1 is crucial in suppression of interference noise. As an example, we consider the detection of subcarrier L_1 at BS1 for the downlink. Due to limited nonadjacent crosstalk suppression of optical filter 1, as shown in Fig. 2, the residual optical carriers $C_1 + C'_3, C'_2$, and $C_2 + C'_4$ may beat with the subcarrier L_1, resulting in crosstalk. Similarly for uplink, nonadjacent crosstalk suppression of optical filter 1 in Fig. 3 will introduce interference noise. As seen in Fig. 7, residual optical carrier C_1 may beat with the subcarrier U_1, resulting in interference in the detection of U_1 at CS. More importantly, the residual optical carrier C_1 may introduce inter-channel crosstalk. If another optical carrier from another channel is located at the same or close wavelength as optical carrier C_1, residual optical carrier C_1 may beat with subcarriers, which is carried by the another optical carrier, resulting in inter-channel interference.

V. Conclusion

A novel RoF system with a DWDM bus architecture has been proposed based on the principle that, for a considered subcarrier, its optical carrier for transmitting is replaced by the other one before detection for downlinks and before optical multiplexing for uplinks. Both of the two optical lasers for each channel are located at CSs, phase locked and polarization aligned, for connecting the CS to each BS. Thus, the proposed RoF system can be immune to laser phase noise. In the downlink system, a low RF signal is used at the CS, and all optical carriers with their subcarriers are multiplexed and transmitted over the downlink fiber. The generation of a millimeter-wave-band RF (such as $\sim$30 GHz) signal for a considered subcarrier at BSs is accomplished by replacing its transmitting optical carrier by the other one, which beats with the considered subcarrier, without the involvement of either the photonic frequency down-conversion, or any electrical frequency mixing technique or the dual-mode light at BSs, or a remote pilot tone at CSs. In the uplink system, a received millimeter-wave-band (such as $\sim$30 GHz) RF signal at BSs is imposed onto two optical carriers simultaneously; one optical carrier with the closest subcarrier, a subcarrier of the other optical carrier, and typically a few gigahertz from the optical carrier, is optically filtered out and fed into the uplink transmission fiber without any optical or electrical conversion. A DWDM demultiplexer directly extracts each optical carrier together with its subcarrier, and a low IF signal, such as $\sim$2 GHz, is directly photodetected at CSs without any electrical or optical frequency conversion. For both downlink and uplink systems, the optical carriers and their subcarriers are not frequency interleaved and, thus, the OSNR and optical modulation depth degradation due to the frequency interleaving is avoided.

Consequently, the proposed RoF system has simple, cost-effective, and maintenance-reduced BSs; and commercially available DWDM multiplexers and demultiplexers can be used. In addition, frequency down-shifting or down-conversion using two phase-locked lasers has been proposed for the first time. Compared to the technique with an MZM or a dual-mode laser with optical heterodyne detection, this technique becomes even simpler. This proposed RoF system can also be used for star-tree and ring architectures. The only drawback of our proposed system is that two polarization maintaining DWDM multiplexers may be required at CSs.

References

[1] P. Smulders, “Exploiting the 60 GHz band for local wireless multimedia access: Prospects and future directions,” *IEEE Commun. Mag.*, pp. 140–147, Jan. 2002.

[2] T. Kuri, K. Kitayama, and Y. Takahashi, “Simplified BS without light source and RF local oscillator in full-duplex millimeter-wave radio-on-fiber system based on external modulation technique,” in *IEEE Int. Microw. Photon. Top. Meeting Tech. Dig.*, 1999, pp. 123–126.

[3] ——, “A single light-source configuration for full-duplex 60-GHz-band radio-on-fiber system,” *IEEE Trans. Microw. Theory Tech.*, vol. 51, no. 2, pp. 431–439, Feb. 2003.

[4] D. Wake, D. Johansson, and D. Moodie, “Passive pico-cell: A new concept in wireless network infrastructure,” *Electron. Lett.*, vol. 33, pp. 404–406, 1997.

[5] G. Smith, D. Novak, and Z. Ahmed, “Overcoming chromatic dispersion effects in fiber-wireless system incorporating external modulators,” *IEEE Trans. Microw. Theory Tech.*, vol. 45, no. 8, pp. 1410–1415, Aug. 1997.

[6] ——, “Technique for optical SSB generation to overcome dispersion penalties in fiber-radio systems,” *Electron. Lett.*, vol. 33, pp. 74–75, 1997.

[7] A. Narasimha, X. Meng, M. Wu, and E. Yablonovitch, “Tandem single sideband modulation scheme for doubling spectral efficiency of analogue fiber links,” *Electron. Lett.*, vol. 36, pp. 1135–1136, 2000.

[8] H. Toda, T. Yamashita, T. Kuri, and K. Kitayama, “Demultiplexing using an arrayed-waveguide grating for frequency-interleaved DWDM millimeter-wave radio-on-fiber systems,” *J. Lightw. Technol.*, vol. 21, no. 8, pp. 1735–1741, Aug. 2003.

[9] T. Kuri, K. Kitayama, and Y. Ogawa, “Fiber-optic millimeter-wave uplink system incorporating remotely fed 60-GHz-band optical pilot tone,” *IEEE Trans. Microw. Theory Tech.*, vol. 47, no. 7, pp. 1332–1337, Jul. 1999.

[10] C. Lim, A. Nirmalathas, D. Novak, R. Waterhouse, and G. Yoffe, “Millimeter-wave broad-band fiber-wireless system incorporating baseband data transmission over fiber and remote LO delivery,” *J. Lightw. Technol.*, vol. 18, no. 10, pp. 1355–1363, Oct. 2000.

[11] C. Lim, A. Nirmalathas, M. Attygalle, D. Novak, and R. Waterhouse, “On the merging of millimeter-wave fiber-radio backbone with 25-GHz WDM ring networks,” *J. Lightw. Technol.*, vol. 21, no. 10, pp. 2203–2210, Oct. 2003.

[12] T. Kuri and K. Kitayama, “Optical heterodyne detection of millimeter-wave-band radio-on-fiber signals with a remote dual-mode local light source,” *IEEE Trans. Microw. Theory Tech.*, vol. 49, no. 10, pp. 2025–2029, Oct. 2001.

[13] ——, “Optical heterodyne detection technique for densely multiplexed millimeter-wave-band radio-on-fiber systems,” *J. Lightw. Technol.*, vol. 21, no. 12, pp. 3167–3179, Dec. 2003.

[14] T. Kuri, H. Toda, and K. Kitayama, “Dense wavelength-division multiplexing millimeter-wave-band radio-on-fiber signal transmission with photonic downconversion,” *J. Lightw. Technol.*, vol. 21, no. 6, pp. 1510–1517, Jun. 2003.

[15] T. Kuri, K. Kitayama, A. Stöhr, and Y. Ogama, “Fiber-optic millimeter-wave downlink system using 60-GHz-band external modulation,” *J. Lightw. Technol.*, vol. 17, no. 5, pp. 799–806, May 1999.

[16] K. Kitayama, “Architectural consideration of radio-on-fiber millimeter-wave wireless access system,” *Fiber Integr. Opt*, vol. 19, pp. 167–186, 2000.

[17] M. Ogusu, K. Inagaki, Y. Mizuguchi, and T. Ohira, “Multiplexing of millimeter-wave signals for fiber-radio links by direct modulation of a two-mode locked Fabry–Pérot laser,” *IEEE Trans. Microw. Theory Tech.*, vol. 52, no. 2, pp. 498–507, Feb. 2004.

[18] K. Ikeda, T. Kuri, and K. Kitayama, “Simultaneous three-band modulation and fiber-optic transmission of 2.5-Gb/s baseband, microwave-, and 60-GHz-band signals on a single wavelength,” *J. Lightw. Technol.*, vol. 21, no. 12, pp. 3194–3202, Dec. 2003.

[19] T. Kamisaka, T. Kuri, and K. Kitayama, “Simultaneous modulation and fiber-optic transmission of 10-Gb/s baseband and 60-GHz-band radio signals on a single wavelength,” *IEEE Trans. Microw. Theory Tech.*, vol. 49, no. 10, pp. 2013–2017, Oct. 2001.

[20] A. Nirmalathas, C. Lim, D. Novak, and R. Waterhouse, “Optical interfaces without light source for base-station designs in fiber-wireless systems incorporated WDM,” in *IEEE Int. Microw. Photon. Top. Meeting Tech. Dig.*, 1999, pp. 119–122.

[21] K. Kitayama, T. Kuri, K. Onohara, T. Kamisaka, and K. Murashima, “Dispersion effects of FBG filter and optical SSB filtering in DWDM millimeter-wave fiber-radio systems,” *J. Lightw. Technol.*, vol. 20, no. 8, pp. 1397–1407, Aug. 2002.

[22] C. Lim, A. Nirmalathas, D. Novak, and R. Waterhouse, “Capacity analysis for WDM fiber-radio backbones with star-tree and ring architecture incorporating wavelength interleaving,” *J. Lightw. Technol.*, vol. 21, no. 12, pp. 3308–3315, Dec. 2003.

[23] G. Smith, D. Novak, and C. Lim, “A millimeter-wave full-duplex fiber-radio star-tree architecture incorporating WDM and SCM,” *IEEE Trans. Microw. Theory Tech.*, vol. 10, no. 11, pp. 1650–1652, Nov. 1998.

[24] M. Attygalle, C. Lim, G. Pendock, A. Nirmalathasa, and G. Edvell, “Transmission improvement in fiber wireless links using fiber Bragg grating,” *IEEE Photon. Technol. Lett.*, vol. 17, no. 1, pp. 190–192, Jan. 2005.

[25] R. Hui, B. Zhu, R. Huang, C. Allen, and K. Demarest, “Subcarrier multiplexing for high speed optical transmission,” *J. Lightw. Technol.*, vol. 20, no. 3, pp. 417–427, Mar. 2002.

[26] T. Kuri, T. Nakasyotani, H. Toda, and K. Kitayama, “Characterization of supercontinuum light source for WDM millimeter-wave-band radio-on-fiber systems,” *IEEE Photon. Technol. Lett.*, vol. 17, no. 6, pp. 1274–1276, Jun. 2005.

Xiupu Zhang (M'00) received the M.Sc. degree from Beijing University of Posts and Telecommunications, Beijing, China in 1988, and the Ph.D. degree from the Technical University of Denmark, Lyngby, Denmark, in 1996, both in electrical engineering.

Following his doctoral study, he became a Research Fellow with the Chalmers University of Technology, Göteborg, Sweden, for one and one half of years. Prior to joining Concordia University, Montréal, QC, Canada, in June 2002, he was involved in the fiber-optics industry in China, Canada, and the U.S. for approximately ten years. He is currently an Associate Professor with Department of Electrical and Computer Engineering, Concordia University. His current research interests include optical fiber transmission, radio-over-fiber systems, fiber amplifiers, and broad-band optical sources.

Dr. Zhang is a member of the Optical Society of America (OSA).

Baozhu Liu, photograph and biography not available at time of publication.

Jianping Yao (M'99–SM'01) received the Ph.D. degree in electrical engineering from the Université de Toulon, Toulon, France, in 1997.

From January 1998 to July 1999, he was a Research Fellow, and from July 1999 to December 2001, he was an Assistant Professor with the School of Electrical and Electronic Engineering, Nanyang Technological University, Singapore. From January 2005 to March 2005, he was an Invited Professor with the Institut National Polytechnique de Grenoble, Grenoble, France. Since December 2001, he has been with the School of Information Technology and Engineering, University of Ottawa, Ottawa, ON, Canada, where is currently an Associate Professor. He has authored or coauthored over 100 papers in refereed journals and conference proceedings. His current research interests include optical signal processing, optically controlled phased-array antennas, photonic generation of microwave signals, radio-over-fiber systems, fiber lasers and amplifiers, broad-band infrared wireless home networking, and fiber-optic sensors.

Dr. Yao is a member of The International Society for Optical Engineers (SPIE) and the Optical Society of America (OSA).

Ke Wu (M'87–SM'92–F'01) is a Professor of electrical engineering and the Tier-I Canada Research Chair in Radio-Frequency and Millimeter-Wave Engineering at the École Polytechnique, Montreal, QC, Canada. He was a Visiting or Guest Professor with many universities around the world. He also holds an honorary visiting professorship and a Cheung Kong endowed chair professorship with Southeast University, Nanjing, China, and an honorary professorship at the Nanjing University of Science and Technology, Nanjing, China. He has been the Director of the Poly-Grames Research Center as well as the Founding Director of the Canadian Facility for Advanced Millimeter-wave Engineering (FAME). He has authored or coauthored over 420 referred papers and several books/book chapters. His current research interests involve substrate integrated circuits, antenna arrays, advanced computer-aided design and modeling techniques, and development of low-cost RF and millimeter-wave transceivers. He is also interested in the modeling and design of microwave photonic circuits and systems. He serves on the Editorial Board of *Microwave Journal*, *Microwave and Optical Technology Letters* and Wiley's *Encyclopedia of RF and Microwave Engineering*. He is an Associate Editor of the *International Journal of RF and Microwave Computer-Aided Engineering*.

Dr. Wu is a Fellow of the Canadian Academy of Engineering (CAE) and the Royal Society of Canada (The Canadian Academy of the Sciences and Humanities) and a member of the Electromagnetics Academy, Sigma Xi, and the URSI. He has held many positions in and has served on various international committees, including the vice chairperson of the Technical Program Committee (TPC) for the 1997 Asia–Pacific Microwave Conference, the general co-chair of the 1999 and 2000 SPIE's International Symposium on Terahertz and Gigahertz Electronics and Photonics, the general chair of the 8th International Microwave and Optical Technology (ISMOT'2001), the TPC Chair of the 2003 IEEE Radio and Wireless Conference (RAWCON'2003), and the general co-chair of the RAWCON'2004. He has served on the Editorial or Review Boards of various technical journals, including the IEEE TRANSACTIONS ON MICROWAVE THEORY AND TECHNIQUES, the IEEE TRANSACTIONS ON ANTENNAS AND PROPAGATION, and the IEEE MICROWAVE AND WIRELESS COMPONENTS LETTERS. He served on the 1996 IEEE Admission and Advancement Committee and the Steering Committee for the 1997 joint IEEE Antennas and Propagation Society (AP-S)/URSI International Symposium. He has also served as a TPC member for the IEEE Microwave Theory and Techniques Society (IEEE MTT-S) International Microwave Symposium. He was elected to the Board of Directors of the Canadian Institute for Telecommunication Research (CITR). He is currently the chair of the joint IEEE chapters of MTTS/APS/LEOS in Montreal, QC, Canada, the chapter coordinator for MTT-S Region 7, and the vice chair of the IEEE MTT-S Transnational Committee. He was the recipient of a URSI Young Scientist Award, the Oliver Lodge Premium Award of the Institute of Electrical Engineer (IEE), U.K., the Asia-Pacific Microwave Prize, the University Research Award "Prix Poly 1873 pour l'Excellence en Recherche" presented by the École Polytechnique on the occasion of its 125th anniversary, the Urgel-Archambault Prize (the highest honor) in the field of physical sciences, mathematics, and engineering from the French-Canadian Association for the Advancement of Science, and the 2004 Fessenden Medal of the IEEE Canada. In 2002, he was the first recipient of the IEEE MTT-S Outstanding Young Engineer Award.

Raman Kashyap, photograph and biography not available at time of publication.